1 **Getting more out of FLAG-Tag co-immunoprecipitation mass spectrometry**

2 **experiments using FAIMS.**

3 **Ching-Seng Ang [*,1], Joanna Sacharz [2], Michael G. Leeming [1], Shuai Nie [1], Swati Varshney [1], Nichollas E.**

4 **Scott [3] and Nicholas A. Williamson [*,1]**

5

6 [1] Bio21 Mass Spectrometry and Proteomics Facility, The University of Melbourne, Parkville, Victoria 3052,

7 Australia

8

9 [2] Department of Biochemistry and Molecular Biology, Bio21 Molecular Science and Biotechnology

10 Institute, University of Melbourne, Parkville, 3052 Victoria, Australia

11

12 [3] Department of Microbiology and Immunology, University of Melbourne at the Peter Doherty Institute

13 for Infection and Immunity, Melbourne 3000

14

15 *Correspondence to Ching-Seng Ang and Nichollas A. Williamson

16 Email: cang@unimelb.edu.au (ORCID ID: 0000-0001-7861-6719) and nawill@unimelb.edu.au (ORCID ID:

17 0000-0002-2173-3452)

18

19 Keywords: Co-IP mass spectrometry, FLAG Tag, FAIMS, ion mobility, Proteomics

20

21

22

23   **Abstract**

24   Co-immunoprecipitation of proteins coupled to mass spectrometry is critical for the understanding of

25   protein interaction networks. In instances where a suitable antibody is not available, it is common to graft

26   synthetic tags onto target protein sequences and allowing the use of commercially available antibodies

27   for affinity purification. A common approach is through FLAG-Tag co-immunoprecipitation. To allow the

28   selective elution of protein complexes, competitive displacement using a large molar excess of the tag

29   peptides is often carried out. Yet, this creates downstream challenges for the mass spectrometry analysis

30   due to the presence of large quantities of these peptides. Here, we demonstrate that Field Asymmetric

31   Ion Mobility Spectrometry (FAIMS), a gas phase ion separation device prior to mass spectrometry analysis

32   can be applied to FLAG-Tag co-immunoprecipitation experiment to increase the depth of protein

33   coverage. By excluding these abundant tag peptides, we were able to observe deeper coverage of

34   interacting proteins and as a result, deeper biological insights, without the need for additional sample

35   handling or altering sample preparation protocols.

36

37   **Introduction**

38   Many studies in systems biology focus on identifying and characterizing protein-protein interactions (PPI)

39   [1, 2]. Co-immunoprecipitation coupled with mass spectrometry (Co-IP/MS) is an extremely powerful

40   analytical technique and has been pivotal in PPI studies to identify protein complexes, co-factors and

41   signaling molecules [3, 4]. Over the last 20 years, Co-IP/MS approaches have evolved from multiple step

42   isolation procedures such as tandem affinity purification [5] to single step protocols [6] to improve the

43   sensitivity, robustness and ability to assess low affinity PPIs. Despite these improvements, the

44   fundamental approach has remained unchanged and are dependent on the use of specific antibodies

45   against a target protein which exists within a protein complex. Using these affinity reagents, immune

46   complexes are captured and interacting proteins identified using mass spectrometry. While there are

47   thousands of commercially available antibodies and with considerable research efforts being directed

48   toward cataloging these antibodies [7], not all affinity reagents are ideal for Co-IPs or are available for all

49   proteins.

50   To circumvent the need for protein specific reagents, a common strategy employed by researchers is to

51   tagged proteins with defined peptide or protein sequences. This involves coupling a small peptide or

52   protein tag to the N- or C-terminus of the target protein to minimize its effect on the protein function.

53   The tagged protein can then be detected using antibodies against the tag sequence rather than the target

54   protein itself. These tag-specific antibodies are available commercially and have been very well

55   characterized for their specificity and sensitivity. Examples of common protein tags include green

56   fluorescent protein (GFP), Glutathione S-Transferase (GST) and mCherry while FLAG, c-Myc, 6X-His and

57   Hemagglutinin (HA) are examples of recombinant peptide tags [8-11]. Proteins interacting with the tagged

58   target can be identified by eluting the interacting proteins from the target protein/antibody complex.

59   There are multiple sample preparation options for the elution step and one common approach is to elute

60   the complex from the affinity beads by using competitive displacement [9, 12] whereby molar excess of a

3

61 synthetic peptide (eg 2X Myc peptide; EQKLISEEDLEQKLISEEDL or 3X FLAG peptide;

62 MDYKDHDGDYKDHDIDYKDDDDK) is added to displace the bound proteins from the tag-specific antibody

63 under non-denaturation conditions. This approach limits the elution of non-specifically bound proteins

64 and allows the elution of complexes in buffers directly compatible with downstream digestion protocols.

65 Unfortunately, the presence of these excess peptides possesses an analytical challenge for subsequent

66 mass spectrometry analysis. Due to the high relative abundances, these 'contaminant' peptides rapidly

67 consume the ion storage capacity of ion trapping devices (C-trap, ion trap etc) [13, 14] and thus artificially

68 reduce the ability to detect other peptides (i.e. those arising from interactor proteins of interest) present

69 in the sample mix.

70 A range of techniques such as gas phased fractionation, BoxCar and Ion mobility (IM) based fractionation

71 [15-18] have been developed that aim to reduce the suppressive effects of highly abundant ions and to

72 increase proteome coverage. Ion mobility mass spectrometry is a technique whereby ions are separated

73 in the gas phase under influence of an electric field. Separation is related to a combination of their size,

74 shape and charge which influence the drift time - the time taken for the molecule to transverse towards

75 the detector [19, 20]. Multiple IM techniques have been developed that differ in the physical principles

76 utilized to achieve ion separation. IM systems can be broadly classified under linear and nonlinear

77 methods [21]. In the linear method, K_0 (reduced mobility) is assumed to be independent of the electric

78 field. These methods include Travelling Wave (TWIMS), Trapped Ion Mobility (TIMS), Drift Tube Ion

79 Mobility (DTIMS) and Differential Mobility Analyzers (DMA). In the nonlinear methods, K (mobility) of any

80 ion in any gas is dependent on the electric field. These methods include Differential Ion Mobility

81 Spectrometry (DIMS) and Field Asymmetric Ion Mobility (FAIMS). Each IM technique has its strengths and

82 are suitable for different applications. The IM systems can help address some of the issue of under

83 sampling due to the stochastic sampling of eluted peptides and bias caused by poor ion selection in a data

84 dependent acquisition methodology [22]. Multiple groups have utilized different forms of ion mobility

4

85   mass spectrometry to increase protein coverage in complex cellular systems [16, 18, 23]. We and others

86   have also used IM to enrich for modified peptides [24-26] or as a targeted SRM-like screening [27]

87   technique. These techniques took advantage of the unique collisional cross sectional properties of the

88   peptides on a linear IM device or by matching the applied compensation voltage of the targeted peptide

89   in a nonlinear FAIMS IM device.

90

91   FAIMS works by having two electrodes with alternating high and low electric field strength across these

92   electrodes. Separation of ions is by differences in their mobility in high and low electric fields [28, 29]. To

93   prevent collision of the ions with the electrode, the ions are diverted through application of a specific DC

94   compensation voltage (CV). The FAIMS device can therefore be used as a filtering device to remove

95   undesirable singly charged and interfering contaminating ions (eg solvent clusters). This allows the ion

96   current to be spread out and limit the proportion of high abundant species that contribute to the maximal

97   charge capacity of the C-trap [13]. The earlier version of the commercially available FAIMS device has met

98   with limited success due to significant ion losses [30]. Modifications to that FAIMS device by the Moritz

99   lab allowed them to be coupled to nanoLC-MS/MS systems, which significantly increased the depth of

100   proteome coverage in a complex yeast digest [31, 32] . The increased in coverage was attributed to the

101   reduction of singly charged chemical noise and resultant increase in the signal to noise of tryptic peptides.

102   More recent publications from the Coon and Thibaut labs using the second generation FAIMS device [16,

103   23] upon coupling them to Orbitrap Fusion Tribrid mass spectrometer show marked increase in protein

104   identification from whole cell lysate by ~10-55% than without FAIMS. Similar to the data shown by the

105   Moritz lab, singly charged species are almost constraint to a small CV range of between -10 and -40, are

106   being diverted and are instrumental in the increase in identification.

107

108   It is evident that FAIMS has the ability to increase proteome coverage in a highly complex sample by using

109   it as a prefiltering device to remove singly charged chemical noise. The benefit of FAIMS however is not

110   just limited to highly complex samples. In this manuscript, we were able to exploit the same prefiltering

111   principal in a FLAG-Tag Co-IP experiment to filter out highly abundant FLAG peptides that exists in multiple

112   charge states. These highly abundant FLAG peptides would otherwise interfere with the detection of the

113   less abundant peptides derived from the affinity target protein and its respective binding proteins. We

114   were able to demonstrate a huge improvement in terms of identified proteins in a supposedly 'simple'

115   Co-IP experiment and the resultant protein-protein interaction network analysis when compared to one

116   without application of FAIMS.

117

118   **Experimental Section**

119   **Affinity Enrichment of Flag-Tag proteins**

120   Affinity enrichment of FLAG-Tag protein experiment was performed from eHap knockout cells or HEK293

121   cells expressing FLAG-Tag protein as described previously [33]. Cell were solubilised in 1% (w/v) digitonin

122   in solubilization buffer (20mM Tris (pH 7.4), 50mM NaCl, 10% (v/v) Glycerol, 0.1 mM EDTA, 5U benzonase

123   (Merck Millipore), 2mM $MgCl_2$). Following clarification of cell lysate by centrifugation (20,000g, 10 mins,

124   4°C), 500 µg protein was added to spin columns (Pierce) containing anti-FLAG M2 affinity resin (Merck)

125   and allowed to incubate rotating for two hours at 4°C. Non-specifically bound proteins were then removed

126   by washing with 20x column volumes of ice-cold solubilization buffer containing 0.1% (w/v) digitonin.

127   Proteins were eluted with 50 µl of 100 µg/mL of 3X FLAG tag peptide (Merck) in solubilization buffer

128   followed by acetone precipitation (overnight, -20°C). Proteins were then pelleted by centrifugation

129   (21,000g, 10 mins, 4°C), washed with ice-cold acetone and air-dried. The pellet was then resolubilised by

130   sonification in with 8M urea in 50 mM ammonium bicarbonate (ABC). Samples were reduced and

6

131   alkylated with 50mM TCEP (ThermoFisher) and 500 mM Chloroacetamide (Merck) (30mins, 37°C,

132   shaking). Elutions were diluted to 2M urea in 50mM ABC and digested in trypsin (Promega) overnight at

133   37°C. The digest was acidified to a final concentration of 1% (v/v) trifluoracetic acid (TFA) and peptides

134   were desalted with stagetips containing 2x plugs of 3M™ Empore™ SDB-XC substrate (SUPELCO). Stagetips

135   were activated with 100% Acetonitrile (ACN) and washed with 0.1% (v/v) TFA, 2% (v/v) ACN prior to

136   binding of peptides. Samples were eluted in 80% ACN, 0.1% TFA and dried completely in a SpeedVac.

137   Peptides were reconstituted in 2% ACN, 0.1% TFA and transferred to autosampler vials for analysis by LC

138   MS/MS

139   **LC MS/MS analysis**

140   LC MS/MS was carried out using the Fusion Lumos Orbitrap mass spectrometers with the FAIMS Pro

141   interface (Thermo Fisher, USA) and as described previously [26]. The LC system was equipped with an

142   Acclaim Pepmap nano-trap column (Dionex-C18, 100 Å, 75 μm x 2 cm) and an Acclaim Pepmap RSLC

143   analytical column (Dionex-C18, 100 Å, 75 μm x 50 cm). Tryptic peptides were injected into the enrichment

144   column at an isocratic flow of 5 μL/min of 2% (v/v) acetonitrile containing 0.1% (v/v) formic acid for 6 min,

145   applied before the enrichment column was switched in-line with the analytical column. The eluents were

146   0.1% (v/v) formic acid (solvent A) in water and 100% (v/v) acetonitrile in 0.1% (v/v) formic acid (solvent

147   B). The flow gradient was (i) 0-6 min at 3% B; (ii) 6-35 min, 3-22% B; (iii) 35-40 min, 22-40% B; (iv) 45-50

148   min, 40-80% B; (v) 50-55 min, 80-80% B; (vi) 55-56 min 85-3% and equilibrated at 3% B for 10 min before

149   injecting the next sample. Tune version 3.3.2782.32 was used. For non-FAIMS experiments, the mass

150   spectrometer was operated in the data-dependent acquisition mode, whereby full MS1 spectra were

151   acquired in a positive mode at 60000 resolution. The 'top speed' acquisition mode with 3 s cycle time on

152   the most intense precursor ion was used, whereby ions with charge states of 2 to 7 were selected.

153   Automated gain control (AGC) target was set to standard with auto maximum injection mode. MS/MS

154   analyses were performed by 1.6 *m/z* isolation with the quadrupole, fragmented by CID with collision

155   energy of 35 %, activation time of 10 ms and activation Q of 0.25. Analysis of fragment ions was carried

156   out in the ion trap using the 'Turbo' speed scanning mode. Dynamic exclusion was activated for 30 s. For

157   FAIMS-enabled experiments, the mass spectrometer was operated in the data-dependent acquisition

158   mode scanning from m/z 300-1600 at 60000 resolution. FAIMS separations were performed with the

159   following settings: inner electrode temperature = 100 °C, outer electrode temperature = 100 °C, FAIMS

160   carrier gas flow = 0 L/min. The FAIMS carrier gas was N_2. Cycle time using the 'top speed acquisition' mode

161   for single CV experiment were 3 s and, for experiments wherin two CVs (-40 and-60) were applied and

162   cycle time was 1.5 s each. MS/MS analyses were performed by 1.6 m/z isolation with the quadrupole,

163   fragmented by CID with collision energy of 35 %, activation time of 10 ms and activation Q of 0.25. Analysis

164   of fragment ions was carried out in the ion trap using the 'Turbo' speed scanning mode. Dynamic exclusion

165   was activated for 30 s.

166

167   For LC MS/MS experiments on an Orbitrap Eclipse the nanoLC conditions were kept constant. The mass

168   spectrometer was operated in the data-dependent acquisition mode, whereby full MS1 spectra were

169   acquired in a positive mode at 60000 resolution. Tune version was 3.3.2782.34. The 'top speed' acquisition

170   mode with 3 s cycle time on the most intense precursor ion was used, whereby ions with charge states of

171   2 to 7 were selected. AGC target was set to standard with auto maximum injection mode. MS/MS analyses

172   were performed by 1.6 m/z isolation with the quadrupole, fragmented by CID with collision energy of 35

173   %, activation time of 35 ms and activation Q of 10. Analysis of fragment ions was carried out in the ion

174   trap using the 'Turbo' speed scanning mode. Dynamic exclusion was activated for 30 s.

175   For LC MS/MS experiments on an Orbitrap Exploris 480, the nanoLC conditions were kept constant. The

176   mass spectrometer was operated in the data-dependent acquisition mode, whereby full MS1 spectra

177   were acquired in a positive mode at 60000 resolution. Tune version was 2.0.182.25. The 'top speed'

8

178   acquisition mode with 3 s cycle time on the most intense precursor ion was used, whereby ions with

179   charge states of 2 to 7 were selected. MS/MS analyses were performed by 1.6 *m/z* isolation with the

180   quadrupole, fragmented by HCD with collision energy of 30%. MS2 resolution was at 15000 Dynamic

181   exclusion was activated for 30 s. AGC target was set to standard with auto maximum injection mode.

182   Dynamic exclusion was activated for 30 s.

183

184   **Database search**

185   Database searches was carried out using Proteome Discoverer (v2.4) with the SequestHT search engine

186   or the Maxquant proteomics software package (version 2.0.1.0) against a *Homo Sapiens* database

187   (SwissProt Taxonomy ID 9606, updated Feb 2021). The SequestHT search parameters are Trypsin as the

188   cleavage enzyme and a maximum of 2 missed cleavages. Precursor and fragment mass tolerances of 10

189   ppm and 0.6 Da, respectively. The default instrument specific search parameters were used in the

190   Maxquant specific searches. For both search engines, carbamidomethyl cysteine was set as fixed

191   modification, and oxidation of methionine and acetylation of the protein N-terminus were considered as

192   variable modifications. Protein and peptides groups were set to a maximum false discovery rate (FDR) of

193   < 0.01 as determined by the Percolator or Maxquant algorithm [34, 35]. Peak area determination was

194   carried out using the Skyline software [36]. Statistical analysis was carried out using the Perseus

195   computational platform [37]. To correct for multiple-hypothesis testing, significant hits are defined using

196   Student's T-test, truncated by permutation-based FDR threshold of 0.05 (250 randomization) and S0

197   factor of 2.0 [38]. Protein-protein interaction network and functional enrichment analysis was performed

198   using STRING [39].

199
200   **Results**

201   The total ion chromatogram (TIC) of a FLAG Co-IP/MS experiment following competitive displacement

202   with 3X FLAG peptide and *in solution* digest is shown in Figure 1A. Three dominant peaks are visible in the

203   chromatogram between 16.0 min and 26 min. The later TIC peak is being dominated by few highly charged

204   ions, corresponding to multiply charged species of the 3X FLAG peptide - MDYKDHDGDYKDHDIDYKDDDDK

205   (2+, 3+, 4+, 5+ and 6+). The earlier TIC peaks consist of a number of modified or truncated versions of the

206   3X FLAG peptide e.g. oxidized methionine, trypsin cleavage products (MDYYK↓DHDGDYKDHDIDYKDDDDK)

207   and the oxidized forms of these tryptic peptides. These high abundant peptides typically co-elute with

208   other tryptic peptides within the 10 min elution window. This result is representative of a large fraction

209   of Co-IP/MS experiments wherein the most abundant ions detected are introduced as byproducts of the

210   assay itself and do not correspond to peptides arising from interactor proteins.

211

212   The most abundant ions observed in each of these major chromatographic peaks correspond to highly

213   charged (+4 to +6) 3X FLAG-derived peptide ions (Figures 1B and 1C). Given that tryptic peptides produced

214   from analyte proteins are most commonly observed in +2 or +3 charge states, the higher charges of the

215   3X FLAG contaminant ions offered the possibility that these could be removed in the gas phase via FAIMS.

216   The synthetic 3X FLAG peptide was first analyzed on the FAIMS/Lumos Orbitrap mass spectrometer with

217   incrementally increasing compensation voltages from CV-20 to CV-70 in steps of 10 (Figure 2). With the

218   exception of the $[M+4H]^{4+}$ precursor at CV-60 and CV-70, all the other charge states of the 3X FLAG were

219   reduced in measured intensity between 30% and 100% (Figure 2, Supplementary Table 1). Next, a FLAG

220   Co-IP experiment was carried out on a whole cell lysate. Following *in solution* digest, the same sample was

221   repeatedly analyzed using the FAIMS/Lumos Orbitrap with the same incrementally increasing

222   compensation voltages to assess the number of proteins, peptides, and peptide spectral matches (PSM)

223   identified under these varying FAIMS conditions. Without FAIMS, 365 proteins, 1362 peptides and 1603

224   PSM were identified (at 1% FDR). The greatest improvement in identifications were when FAIMS was

225   operated with a CV of -40. This led to gains of 93%, 58% and 51% in proteins, peptides and PSM,

226   respectively, as compared to analysis of the same sample without FAIMS (Figure 3A). The remainder of

227   the single CVs tested led to either comparable (CV- 30 and -50) or substantially lower (CV -20, -60, -70)

228   proteins, peptides and PSM upon database searching.

229

230   While the greatest improvement in protein identifications was observed for CV-40, it is well documented

231   that different, and perhaps complementary, subsets of peptides may be preferentially detected at

232   alternative CVs or internal CV stepping [23]. To assess whether identification numbers may be improved

233   by employing internal CV stepping, the same FLAG Co-IP digest was re-analyzed with two internal CV steps

234   of -40 and -60. Here, 734 proteins, 2550 peptides and 2904 PSMs were identified following database

235   searching. This translates to a 100%, 59% and 81% gain as compared to without FAIMS. This is almost a 2-

236   fold increase in the total protein identification but critically, the number of proteins that was exclusively

237   identified in the FAIMS experiment was 409 when two internal CV stepping were applied as compared to

238   only 40 without FAIMS (Figure 3D). The distribution of the different charge species selected for MS/MS

239   follows a trend of decreasing 2+ peptides and increasing 4+ and 5+ peptides with more negative CVs

240   (Figure 3E). 3+ peptides appear to be uniformly distributed and within ~20%-45% of all measured MS1

241   features across CV-30 to CV-70. We repeated this experiment on an independent FLAG Co-IP experiment

242   targeting a different FLAG-Tag protein, and observed similar and large increase in the protein, peptide

243   and PSM (Supplementary Figure 1).

244

245   The TIC and number of PSM identifications were plotted across the HPLC retention time at the regions

246   (16-26min) corresponding to the elution time of the 3X FLAG peptides (Figure 1). With FAIMS rapidly

247   switching between CVs of -40 and -60 FAIMS, there is a noticeable drop in the MS1 ion injection time and

11

248   a corresponding increase in the identified PSM (Figure 4B and 4C). At those alternating CV values, the 5+,

249   6+ charged species and also a large percentage of the 4+ charged species can be effectively reduced or

250   removed (Figure 2), which otherwise would have contributed to filling up a portion of the limited charge

251   capacity of the C-trap. The total number of identified PSM between the 16-26 minute elution window at

252   CV-40 and CV-60 is 374 and 115, respectively. Without FAIMS, the total number of identified PSM is only

253   120.

254

255   To determine if sample complexity has a large effect on protein and peptide identification on the Orbitrap

256   Lumos, a commercial Hela tryptic digest (100ng on column) was analyzed using two internal CV stepping

257   (-40 and -60) and without FAIMS. With FAIMS, 37% and 23% more proteins and peptides, respectively,

258   were identified as compared to without FAIMS. To determine if the increase in identification is not due to

259   the analytical mass spectrometer, the FLAG Co-IP digest was analyzed on the next generation Orbitrap

260   Eclipse and Orbitrap Exploris 480 mass spectrometer using similar LC-MS/MS conditions. The results were

261   then compared with the same FLAG Co-IP digest analyzed on the FAIMS/Lumos Orbitrap with two CV

262   internal stepping (-40 and -60). With FAIMS/Lumos Orbitrap, 70.7% and 114.9% more proteins were

263   identified compared to Eclipse and Exploris 480, respectively. On the peptide level, there were 43.3% and

264   81.1% more from FAIMS/Lumos compared to Eclipse and Exploris 480, respectively (Supplementary Table

265   2).

266

267   All the above Co-IP experiment were carried using the same *in solution* digested sample and comparing

268   protein and peptide identifications, with and without FAIMS. We sought to see if the improvement were

269   indeed biologically relevant in a comparative Co-IP experiment. For this, a FLAG-Tag transmembrane

270   protein was used for immunoprecipitation of proteins after treatment with a drug that targets the

12

271   membrane ion channel. All experiment were performed in triplicates and the *in solution* digested samples

272   were analyzed on the Lumos Orbitrap mass spectrometer with and without FAIMS. After subtracting

273   proteins identified from the negative controls, statistical analysis was carried out to highlight proteins that

274   were significantly changed in abundances upon drug treatment (Figures 5A and 5B). These significantly

275   changed proteins were combined with proteins that are identified exclusively from the drug treatment

276   group (identified in all 3 replicates in drug treatment and absent in all the non-treatment replicates). From

277   the above selection criteria, a list of 265 proteins with FAIMS and 117 proteins without FAIMS was

278   generated (Supplementary Table 3). Protein-protein interaction network and functional enrichment

279   analysis was then carried using STRING (Figures 5D and 5E). We applied the highest confidence score

280   (0.900) and display only edges from where proteins are part of a physical complex (STRING physical

281   subnetworks feature). From these, a highly significant protein-protein interaction (PPI) enrichment for

282   both Co-IP with FAIMS (PPI enrichment p value <1.0e-16) and without FAIMS (PPI enrichment p value =

283   1.3e-11) was obtained. For clarity, the disconnected nodes in the network were not displayed. There are

284   a total of 51 protein (86 edges) enriched from known physical complexes with FAIMS versus 18 proteins

285   (17 edges) from without FAIMS. The top 2 molecular function enrichment from both FAIMS and without

286   FAIMS were related to SNAP receptor (red bubble) and SNARE binding (blue bubble). The endomembrane

287   system (green bubble) was the topmost enriched subcellular localization for both FAIMS and without

288   FAIMS Co-IP experiment.

289

290   **Discussion**

291   Given that FLAG-Tag Co-IP experiments typically produce large molar excesses of contaminant peptides

292   derived from peptides used in competitive displacement, we reasoned that deeper profiling of interacting

293   species could be achieved by developing methods to reduce the suppressive effects of high-abundance

13

294   ions on mass spectrometric detection of low-abundance species. We have utilized FAIMS as a gas phase

295   filtering technique, to filter or reduce the highly abundant synthetic 3X FLAG peptides in a FLAG Co-IP

296   mass spectrometry experiment and have increased the depth of proteome coverage. The total numbers

297   of proteins identified from FLAG-Tag Co-IPs increased two-fold when FAIMS filtering was employed with

298   two, rapid compensation voltage steps (-40 and -60) compared to analyses of the same sample when

299   FAIMS was not used. Critically, a much larger number of proteins were exclusively identified with the

300   application of the optimal FAIMS-filtering method versus when no FAIMS is used.

301

302   It should be noted that a range of techniques are currently available to reduce interference from high-

303   abundance peptides. For example, the excess FLAG peptides could be removed with an offline cleanup

304   process or by running it off an SDS PAGE gel, size exclusion columns, molecular weight filtration etc. The

305   downside is that it requires additional offline sample handling steps and will likely introduce experimental

306   variabilities. A single LC MS/MS experiment with increased depth is still the preferred methodology in a

307   Co-IP/MS experiment. In contrast to these existing methods, the FAIMS methodology presented here does

308   not require any additional sample handling steps, fractionation or library construction and is completely

309   amenable to standard, single-shot data-dependent acquisition.

310

311   We reasoned that one of the largest contributing factors to the increased protein identification is that

312   FAIMS can divert singly charged chemical noise, resulting in increased signal to noise as also demonstrated

313   in earlier studies [16, 23, 31, 32]. Not allowing a few abundant peptides, such as the synthetic 3X FLAG

314   peptide fill up the limited charge capacity of the ion storage device is another significant contributing

315   factor. The later phenomenon has been exploited to increase the proteome coverage in other gas phase

316   fractionation strategies [15, 17, 40]. For example, in the more recent BoxCar acquisition strategy [17], ion

14

317   injection is limited to a portion of the total mass range so as to distribute the maximal charge capacity.

318   This is to limit the proportion of highly abundant or well ionizing peptides affecting ion accumulation in

319   the C-traps, which typically can be filled up in less than 1ms [13]. One millisecond is typically less than 1%

320   of the transient time required to generate a high-resolution mass spectrum in the Orbitrap, which takes

321   between 128-256ms (resolution dependent). What that means is >99% of these ions are not being used

322   for mass analysis. When scanning in limited mass ranges, these gas phased fractionation methodologies

323   can spread out the abundant species which otherwise rapidly fill up the C-trap, thus allowing increased

324   filling time for the less abundant peptides. Although the MS1 overhead and duty is increased with multiple

325   m/z windows, the overall benefits in terms of increased identification of low-level peptides is substantial

326   with up to a 10-fold gain in dynamic range [17]. In a FLAG Co-IP experiment, the presence of the high

327   abundant synthetic 3X FLAG peptide will rapidly fill up the C-trap and can affect accumulation of other

328   low abundant peptides. We have empirically determined the relationship between the applied CV and the

329   charged characteristic for the 3X FLAG peptide (Figure 2). By applying different FAIMS CVs, gas phased

330   fractionation can be used to filter out the high abundant 3X FLAG peptides at different charge states. The

331   charge distribution and mass to charge ratio (m/z) of precursor peptides across multiple CVs in a complex

332   Hela and yeast digest have previously been reported [23, 31, 32]. In addition to the charge states,

333   precursor mass to charge ratio (m/z) also have a large impact on the FAIMS mobility. Optimal

334   compensation field (Ec) for multiply charged peptides varies and the largest m/z are generally observed

335   over lower magnitude Ec and smaller m/z generally over higher Ec and are charge state dependent [32].

336   The reported Co-IP data is in general agreement with the complex digest reported in the earlier

337   investigations, with doubly charged precursors found predominantly at the lower CV, triple charged

338   precursors distributed over a wider CV and higher charge densities observed for more negative CVs.

339

15

340   When performing that as a single LC-MS/MS experiment and two internal CV stepping, a large proportion

341   of the intense 4+, 5+ and 6+ FLAG peptide is filtered at the CV-40 step. This allows gas phase enrichment

342   of the lower charged state peptides derived from the affinity target protein and its respective binding

343   proteins. When switching to the CV-60 step, the characteristics of the peptides differs, allowing

344   identification of a different set of peptides. This is also evident by the decreased MS1 TIC and

345   corresponding increased PSM during the 16-26 minute elution window of the synthetic 3X FLAG peptide

346   (Figure 4). In contrast to the BoxCar acquisition strategy, the minimal increased in MS1 overhead in a

347   FAIMS type experiment has lower impact on the overall instrument duty cycle as only 2 internal CV

348   stepping are used, and the complexity of Co-IP experiment is generally not high.

349

350   We sought to establish if the large increase in protein and peptide identifications is a phenomenon that

351   is augmented in Co-IP experiment and not due to sample complexity or instrumentation. To do that, the

352   differences in identifications using a highly complex whole cell digest with and without FAIMS was carried

353   out. In a complex whole cell digest and using FAIMS, there were 37% and 23% more proteins and peptides

354   identified, respectively, than without FAIMS (Supplementary Table 2). This is in general agreement with

355   the work published by the Coon lab [23] where they showed FAIMS (different CVs compared to this

356   manuscript) providing similar increase in protein identification with the same 60 min analysis time. In the

357   FAIMS Flag-Tag Co-IP experiment, where sample complexity is much lower, there is a 100% and 59%

358   increase in proteins and peptides, respectively. This suggests, removal of singly charged chemical noise

359   and high abundant contaminant 3X FLAG peptides can have a more profound effect in samples of lesser

360   complexity. The same Co-IP experiment was then analyzed without FAIMS on the Orbitrap Lumos and 2

361   newer Orbitraps (Orbitrap Eclipse and Exploris 480) to determine if the same increase in protein and

362   peptide identifications can be achieved with newer instrumentation. The number of identified proteins,

363   peptides and PSM was similar between Orbitrap Eclipse and Lumos and Exploris 480 having the least

364   number of identifications (supplementary Table 2). Again, when comparing all 3 experiments with

365   FAIMS/Lumos, protein, peptide and PSM identification are much higher when FAIMS was used. The

366   Orbitrap Eclipse and Exploris 480 are to date, the latest generation Orbitrap mass spectrometer with

367   improvement in the quad filter, FTMS overheads and better ion transmission [41, 42]. These newer

368   generation of Orbitrap mass spectrometers have been shown to increase the identification rates of

369   proteins as compared to the Fusion Lumos Orbitrap by up to 20% in a complex Hela digest or single cell

370   proteome study where sensitivity is of upmost importance [41, 43]. The much higher protein and peptide

371   identifications clearly shows the increase identification on FAIMS/Lumos cannot be replicated with newer

372   instrumentation. The FAIMS device can provide increased depth in a highly complex sample but for a

373   relatively low complexity sample like a Co-IP experiment, the improvement afforded by filtering out the

374   dominating ion species is much greater.

375   Lastly, we look into the STRING protein-protein interaction networks generated from identified proteins

376   with and without FAIMS. It quickly became apparent that the network generated from the FAIMS dataset

377   is denser, more informative and has more proteins identified than without FAIMS (Figure 5C). Whilst not

378   focusing on any biological interpretation, we sought to find out what gains were achieved. Instead of

379   presenting indirect (functional) interactions where the PPI network can become overly dense and with

380   boundless overlapping nodes, these networks are reported as a more conservative physical subnetwork.

381   This allow us to look at proteins that are experimentally shown to be physically linked and without the

382   added complications of functional interactions derived from computational means [44]. For added clarity,

383   disconnected nodes are also removed from the analysis. With FAIMS, there are 51 proteins that are

384   connected through direct physical interactions versus 17 without FAIMS. The vast majority of these

385   proteins are associated with the endomembrane system, which correlates well with the bait protein being

386   a transmembrane protein. The top 2 enriched molecular function from the FAIMS and no FAIMS dataset

387   are similar and are related to SNARE binding and SNAP receptor activity. SNARE (or SNAP REceptor)

17

388   proteins are made up of a large protein superfamily of more than 60 members in mammalian cells and

389   are involved in membrane fusion along the secretory and endomembrane systems [45]. Although analysis

390   without FAIMS showed similar enrichment in molecular functions, more proteins from the SNARE

391   complexes such as Syntaxins (STX), STXBP, VTI1B, VAMP, SNAP, SEC22A, GOSR2 and RAB [46] are enriched

392   with FAIMS. These SNARE proteins are on top of many more interacting proteins, especially those

393   associated with the endomembrane systems (Figure 4D, green bubble). Being able to identify different

394   STX proteins can provide us with additional information on the cellular localization of these complexes.

395   For example, different members of the SNARE proteins are distributed in distinct subcellular localization,

396   which form specific SNARE complexes to mediate different transport events [46]. 9 different STX proteins

397   versus 3 STX proteins were identified from FAIMS and without FAIMS, respectively. STX5 is present in at

398   least three different SNAREpins, regulating Golgi trafficking and is thought to be the master SNARE of the

399   Golgi apparatus [47]. STX6 and STX16 form one of two Golgi SNAREpins with VTILA and VAMP4 [48].

400   Consolidating the above information allow us to speculate an enhanced interaction of the Golgi network

401   with the transmembrane protein, upon treatment with the membrane ion channel drug. That cannot be

402   said with the Co-IP experiment analyzed without FAIMS. We cannot discount there are also proteins that

403   are uniquely identified from the without FAIMS experiment, but the large increase in protein identification

404   and resultant denser PPI network represents the extension of the depth of proteome coverage, potentially

405   revealing previously unknown protein partners and in our view should be the method of choice for such

406   experiment.

407   Discovery and functional characterization of protein-protein interaction network is challenging. This

408   requires sound experimental planning, the right bait protein(s), high yield of bait proteins and in-depth

409   identification of the interacting proteins. While a full biological analysis of these entities is beyond the

410   scope of this manuscript, these proteins differentially detected with FAIMS could potentially be missing

411   links in protein complexes or low level transient interactors etc. While FAIMS enabled methodology has

412   already been documented to increase proteome coverage for complex proteomics samples we show here

413   that it can have a proportionately greater impact on "simple" or low complexity samples.

414

415   **Data Availability**

416   The mass spectrometry proteomics data have been deposited to the ProteomeXchange Consortium via

417   the PRIDE partner repository with the dataset identifier PXD028965

418

419   **Author Contributions**

420   CSA and NAW designed the research, CSA developed methodology, CSA, MGL, SN, SV performed

421   experiments, all authors analyzed data and wrote the paper.

422

423   **Supporting information**

424   Supplementary data to this article can be found online at …

425

426   **Supplementary Figure 1:** Analyzing the protein and peptide identification from a second independent

427   FLAG Co-IP experiment.

428   **Supplementary Table 1:** Comparing intensities of the different charge states of the 3X FLAG peptide across

429   different CVs.

430

431   **Supplementary Table 2:** Comparing the identification rate across 3 different Orbitrap Mass Spectrometers
432

433   Supplementary Table 3: List of significantly changed proteins used for STRING analysis

434

435   **References**

436

437   [1] T. Rolland, M. Tasan, B. Charloteaux, S.J. Pevzner, Q. Zhong, N. Sahni, S. Yi, I. Lemmens, C. Fontanillo,
438   R. Mosca, A. Kamburov, S.D. Ghiassian, X. Yang, L. Ghamsari, D. Balcha, B.E. Begg, P. Braun, M. Brehme,
439   M.P. Broly, A.R. Carvunis, D. Convery-Zupan, R. Corominas, J. Coulombe-Huntington, E. Dann, M. Dreze,
440   A. Dricot, C. Fan, E. Franzosa, F. Gebreab, B.J. Gutierrez, M.F. Hardy, M. Jin, S. Kang, R. Kiros, G.N. Lin, K.
441   Luck, A. MacWilliams, J. Menche, R.R. Murray, A. Palagi, M.M. Poulin, X. Rambout, J. Rasla, P. Reichert,
442   V. Romero, E. Ruyssinck, J.M. Sahalie, A. Scholz, A.A. Shah, A. Sharma, Y. Shen, K. Spirohn, S. Tam, A.O.
443   Tejeda, S.A. Trigg, J.C. Twizere, K. Vega, J. Walsh, M.E. Cusick, Y. Xia, A.L. Barabasi, L.M. Iakoucheva, P.
444   Aloy, J. De Las Rivas, J. Tavernier, M.A. Calderwood, D.E. Hill, T. Hao, F.P. Roth, M. Vidal, A proteome-
445   scale map of the human interactome network, Cell 159(5) (2014) 1212-1226.
446   [2] P.C. Havugimana, G.T. Hart, T. Nepusz, H. Yang, A.L. Turinsky, Z. Li, P.I. Wang, D.R. Boutz, V. Fong, S.
447   Phanse, M. Babu, S.A. Craig, P. Hu, C. Wan, J. Vlasblom, V.U. Dar, A. Bezginov, G.W. Clark, G.C. Wu, S.J.
448   Wodak, E.R. Tillier, A. Paccanaro, E.M. Marcotte, A. Emili, A census of human soluble protein complexes,
449   Cell 150(5) (2012) 1068-81.
450   [3] R.B. Free, L.A. Hazelwood, D.R. Sibley, Identifying novel protein-protein interactions using co-
451   immunoprecipitation and mass spectroscopy, Curr Protoc Neurosci Chapter 5 (2009) Unit 5 28.
452   [4] K. Markham, Y. Bai, G. Schmitt-Ulms, Co-immunoprecipitations revisited: an update on experimental
453   concepts and their implementation for sensitive interactome investigations of endogenous proteins,
454   Anal Bioanal Chem 389(2) (2007) 461-73.
455   [5] G. Rigaut, A. Shevchenko, B. Rutz, M. Wilm, M. Mann, B. Seraphin, A generic protein purification
456   method for protein complex characterization and proteome exploration, Nat Biotechnol 17(10) (1999)
457   1030-2.
458   [6] E.C. Keilhauer, M.Y. Hein, M. Mann, Accurate protein complex retrieval by affinity enrichment mass
459   spectrometry (AE-MS) rather than affinity purification mass spectrometry (AP-MS), Mol Cell Proteomics
460   14(1) (2015) 120-35.
461   [7] M. Uhlen, L. Fagerberg, B.M. Hallstrom, C. Lindskog, P. Oksvold, A. Mardinoglu, A. Sivertsson, C.
462   Kampf, E. Sjostedt, A. Asplund, I. Olsson, K. Edlund, E. Lundberg, S. Navani, C.A. Szigyarto, J. Odeberg, D.
463   Djureinovic, J.O. Takanen, S. Hober, T. Alm, P.H. Edqvist, H. Berling, H. Tegel, J. Mulder, J. Rockberg, P.
464   Nilsson, J.M. Schwenk, M. Hamsten, K. von Feilitzen, M. Forsberg, L. Persson, F. Johansson, M. Zwahlen,
465   G. von Heijne, J. Nielsen, F. Ponten, Proteomics. Tissue-based map of the human proteome, Science
466   347(6220) (2015) 1260419.
467   [8] S. Munro, H.R. Pelham, Use of peptide tagging to detect proteins expressed from cloned genes:
468   deletion mapping functional domains of Drosophila hsp 70, EMBO J 3(13) (1984) 3087-93.
469   [9] R. Hernan, K. Heuermann, B. Brizzard, Multiple epitope tagging of expressed proteins for enhanced
470   detection, Biotechniques 28(4) (2000) 789-93.
471   [10] J. DeCaprio, T.O. Kohl, Tandem Immunoaffinity Purification Using Anti-FLAG and Anti-HA Antibodies,
472   Cold Spring Harb Protoc 2019(2) (2019).
473   [11] A. Louche, S.P. Salcedo, S. Bigot, Protein-Protein Interactions: Pull-Down Assays, Methods Mol Biol
474   1615 (2017) 247-255.
475   [12] H.R. Hoogenboom, A.D. Griffiths, K.S. Johnson, D.J. Chiswell, P. Hudson, G. Winter, Multi-subunit
476   proteins on the surface of filamentous phage: methodologies for displaying antibody (Fab) heavy and
477   light chains, Nucleic Acids Res 19(15) (1991) 4133-7.

478 [13] R.A. Zubarev, A. Makarov, Orbitrap mass spectrometry, Anal Chem 85(11) (2013) 5288-96.

479 [14] D.J. Douglas, A.J. Frank, D. Mao, Linear ion traps in mass spectrometry, Mass Spectrom Rev 24(1)
480 (2005) 1-29.

481 [15] E.C. Yi, M. Marelli, H. Lee, S.O. Purvine, R. Aebersold, J.D. Aitchison, D.R. Goodlett, Approaching
482 complete peroxisome characterization by gas-phase fractionation, Electrophoresis 23(18) (2002) 3205-
483 16.

484 [16] S. Pfammatter, E. Bonneil, F.P. McManus, S. Prasad, D.J. Bailey, M. Belford, J.J. Dunyach, P. Thibault,
485 A Novel Differential Ion Mobility Device Expands the Depth of Proteome Coverage and the Sensitivity of
486 Multiplex Proteomic Measurements, Mol Cell Proteomics 17(10) (2018) 2051-2067.

487 [17] F. Meier, P.E. Geyer, S. Virreira Winter, J. Cox, M. Mann, BoxCar acquisition method enables single-
488 shot proteomics at a depth of 10,000 proteins in 100 minutes, Nat Methods 15(6) (2018) 440-448.

489 [18] F. Meier, A.D. Brunner, S. Koch, H. Koch, M. Lubeck, M. Krause, N. Goedecke, J. Decker, T. Kosinski,
490 M.A. Park, N. Bache, O. Hoerning, J. Cox, O. Rather, M. Mann, Online Parallel Accumulation-Serial
491 Fragmentation (PASEF) with a Novel Trapped Ion Mobility Mass Spectrometer, Mol Cell Proteomics
492 17(12) (2018) 2534-2545.

493 [19] J.N. Dodds, E.S. Baker, Ion Mobility Spectrometry: Fundamental Concepts, Instrumentation,
494 Applications, and the Road Ahead, J Am Soc Mass Spectrom 30(11) (2019) 2185-2195.

495 [20] F. Lanucara, S.W. Holman, C.J. Gray, C.E. Eyers, The power of ion mobility-mass spectrometry for
496 structural characterization and the study of conformational dynamics, Nat Chem 6(4) (2014) 281-94.

497 [21] V. Gabelica, A.A. Shvartsburg, C. Afonso, P. Barran, J.L.P. Benesch, C. Bleiholder, M.T. Bowers, A.
498 Bilbao, M.F. Bush, J.L. Campbell, I.D.G. Campuzano, T. Causon, B.H. Clowers, C.S. Creaser, E. De Pauw, J.
499 Far, F. Fernandez-Lima, J.C. Fjeldsted, K. Giles, M. Groessl, C.J. Hogan, Jr., S. Hann, H.I. Kim, R.T.
500 Kurulugama, J.C. May, J.A. McLean, K. Pagel, K. Richardson, M.E. Ridgeway, F. Rosu, F. Sobott, K.
501 Thalassinos, S.J. Valentine, T. Wyttenbach, Recommendations for reporting ion mobility Mass
502 Spectrometry measurements, Mass Spectrom Rev 38(3) (2019) 291-320.

503 [22] D.L. Tabb, L. Vega-Montoto, P.A. Rudnick, A.M. Variyath, A.J. Ham, D.M. Bunk, L.E. Kilpatrick, D.D.
504 Billheimer, R.K. Blackman, H.L. Cardasis, S.A. Carr, K.R. Clauser, J.D. Jaffe, K.A. Kowalski, T.A. Neubert,
505 F.E. Regnier, B. Schilling, T.J. Tegeler, M. Wang, P. Wang, J.R. Whiteaker, L.J. Zimmerman, S.J. Fisher,
506 B.W. Gibson, C.R. Kinsinger, M. Mesri, H. Rodriguez, S.E. Stein, P. Tempst, A.G. Paulovich, D.C. Liebler, C.
507 Spiegelman, Repeatability and reproducibility in proteomic identifications by liquid chromatography-
508 tandem mass spectrometry, J Proteome Res 9(2) (2010) 761-76.

509 [23] A.S. Hebert, S. Prasad, M.W. Belford, D.J. Bailey, G.C. McAlister, S.E. Abbatiello, R. Huguet, E.R.
510 Wouters, J.J. Dunyach, D.R. Brademan, M.S. Westphall, J.J. Coon, Comprehensive Single-Shot Proteomics
511 with FAIMS on a Hybrid Orbitrap Mass Spectrometer, Anal Chem 90(15) (2018) 9529-9537.

512 [24] S. Pfammatter, E. Bonneil, F.P. McManus, P. Thibault, Gas-Phase Enrichment of Multiply Charged
513 Peptide Ions by Differential Ion Mobility Extend the Comprehensiveness of SUMO Proteome Analyses, J
514 Am Soc Mass Spectrom 29(6) (2018) 1111-1124.

515 [25] C.D. Chouinard, G. Nagy, I.K. Webb, T. Shi, E.S. Baker, S.A. Prost, T. Liu, Y.M. Ibrahim, R.D. Smith,
516 Improved Sensitivity and Separations for Phosphopeptides using Online Liquid Chromotography Coupled
517 with Structures for Lossless Ion Manipulations Ion Mobility-Mass Spectrometry, Anal Chem 90(18)
518 (2018) 10889-10896.

519 [26] A.R. Ahmad Izaham, C.S. Ang, S. Nie, L.E. Bird, N.A. Williamson, N.E. Scott, What Are We Missing by
520 Using Hydrophilic Enrichment? Improving Bacterial Glycoproteome Coverage Using Total Proteome and
521 FAIMS Analyses, J Proteome Res 20(1) (2021) 599-612.

522 [27] K.E. Burnum-Johnson, S. Nie, C.P. Casey, M.E. Monroe, D.J. Orton, Y.M. Ibrahim, M.A. Gritsenko,
523 T.R. Clauss, A.K. Shukla, R.J. Moore, S.O. Purvine, T. Shi, W. Qian, T. Liu, E.S. Baker, R.D. Smith,
524 Simultaneous Proteomic Discovery and Targeted Monitoring using Liquid Chromatography, Ion Mobility
525 Spectrometry, and Mass Spectrometry, Mol Cell Proteomics 15(12) (2016) 3694-3705.

526   [28] B.M. Kolakowski, Z. Mester, Review of applications of high-field asymmetric waveform ion mobility
527   spectrometry (FAIMS) and differential mobility spectrometry (DMS), Analyst 132(9) (2007) 842-64.
528   [29] K.E. Swearingen, R.L. Moritz, High-field asymmetric waveform ion mobility spectrometry for mass
529   spectrometry-based proteomics, Expert Rev Proteomics 9(5) (2012) 505-17.
530   [30] S. Prasad, M.W. Belford, J.J. Dunyach, R.W. Purves, On an aerodynamic mechanism to enhance ion
531   transmission and sensitivity of FAIMS for nano-electrospray ionization-mass spectrometry, J Am Soc
532   Mass Spectrom 25(12) (2014) 2143-53.
533   [31] K.E. Swearingen, M.R. Hoopmann, R.S. Johnson, R.A. Saleem, J.D. Aitchison, R.L. Moritz, Nanospray
534   FAIMS fractionation provides significant increases in proteome coverage of unfractionated complex
535   protein digests, Mol Cell Proteomics 11(4) (2012) M111 014985.
536   [32] K.E. Swearingen, J.M. Winget, M.R. Hoopmann, U. Kusebauch, R.L. Moritz, Decreased Gap Width in
537   a Cylindrical High-Field Asymmetric Waveform Ion Mobility Spectrometry Device Improves Protein
538   Discovery, Anal Chem 87(24) (2015) 12230-7.
539   [33] D.H. Hock, B. Reljic, C.S. Ang, L. Muellner-Wong, H.S. Mountford, A.G. Compton, M.T. Ryan, D.R.
540   Thorburn, D.A. Stroud, HIGD2A is Required for Assembly of the COX3 Module of Human Mitochondrial
541   Complex IV, Mol Cell Proteomics 19(7) (2020) 1145-1160.
542   [34] L. Kall, J.D. Canterbury, J. Weston, W.S. Noble, M.J. MacCoss, Semi-supervised learning for peptide
543   identification from shotgun proteomics datasets, Nat Methods 4(11) (2007) 923-5.
544   [35] S. Tyanova, T. Temu, J. Cox, The MaxQuant computational platform for mass spectrometry-based
545   shotgun proteomics, Nat Protoc 11(12) (2016) 2301-2319.
546   [36] B. MacLean, D.M. Tomazela, N. Shulman, M. Chambers, G.L. Finney, B. Frewen, R. Kern, D.L. Tabb,
547   D.C. Liebler, M.J. MacCoss, Skyline: an open source document editor for creating and analyzing targeted
548   proteomics experiments, Bioinformatics 26(7) (2010) 966-8.
549   [37] S. Tyanova, T. Temu, P. Sinitcyn, A. Carlson, M.Y. Hein, T. Geiger, M. Mann, J. Cox, The Perseus
550   computational platform for comprehensive analysis of (prote)omics data, Nat Methods 13(9) (2016)
551   731-40.
552   [38] V.G. Tusher, R. Tibshirani, G. Chu, Significance analysis of microarrays applied to the ionizing
553   radiation response, Proc Natl Acad Sci U S A 98(9) (2001) 5116-21.
554   [39] D. Szklarczyk, A.L. Gable, D. Lyon, A. Junge, S. Wyder, J. Huerta-Cepas, M. Simonovic, N.T. Doncheva,
555   J.H. Morris, P. Bork, L.J. Jensen, C.V. Mering, STRING v11: protein-protein association networks with
556   increased coverage, supporting functional discovery in genome-wide experimental datasets, Nucleic
557   Acids Res 47(D1) (2019) D607-D613.
558   [40] B.K. Erickson, D.K. Schweppe, Q. Yu, R. Rad, W. Haas, G.C. McAlister, S.P. Gygi, Parallel Notched Gas-
559   Phase Enrichment for Improved Proteome Identification and Quantification with Fast Spectral
560   Acquisition Rates, J Proteome Res 19(7) (2020) 2750-2757.
561   [41] Q. Yu, J.A. Paulo, J. Naverrete-Perea, G.C. McAlister, J.D. Canterbury, D.J. Bailey, A.M. Robitaille, R.
562   Huguet, V. Zabrouskov, S.P. Gygi, D.K. Schweppe, Benchmarking the Orbitrap Tribrid Eclipse for Next
563   Generation Multiplexed Proteomics, Anal Chem 92(9) (2020) 6478-6485.
564   [42] D.B. Bekker-Jensen, A. Martinez-Val, S. Steigerwald, P. Ruther, K.L. Fort, T.N. Arrey, A. Harder, A.
565   Makarov, J.V. Olsen, A Compact Quadrupole-Orbitrap Mass Spectrometer with FAIMS Interface
566   Improves Proteome Coverage in Short LC Gradients, Mol Cell Proteomics 19(4) (2020) 716-729.
567   [43] Y. Cong, Y. Liang, K. Motamedchaboki, R. Huguet, T. Truong, R. Zhao, Y. Shen, D. Lopez-Ferrer, Y.
568   Zhu, R.T. Kelly, Improved Single-Cell Proteome Coverage Using Narrow-Bore Packed NanoLC Columns
569   and Ultrasensitive Mass Spectrometry, Anal Chem 92(3) (2020) 2665-2671.
570   [44] B. VanderSluis, M. Costanzo, M. Billmann, H.N. Ward, C.L. Myers, B.J. Andrews, C. Boone,
571   Integrating genetic and protein-protein interaction networks maps a functional wiring diagram of a cell,
572   Curr Opin Microbiol 45 (2018) 170-179.

573   [45] J. Han, K. Pluhackova, R.A. Bockmann, The Multifaceted Role of SNARE Proteins in Membrane
574   Fusion, Front Physiol 8 (2017) 5.
575   [46] W. Hong, S. Lev, Tethering the assembly of SNARE complexes, Trends Cell Biol 24(1) (2014) 35-43.
576   [47] J. Malsam, T.H. Sollner, Organization of SNAREs within the Golgi stack, Cold Spring Harb Perspect
577   Biol 3(10) (2011) a005249.
578   [48] O. Laufman, W. Hong, S. Lev, The COG complex interacts directly with Syntaxin 6 and positively
579   regulates endosome-to-TGN retrograde transport, J Cell Biol 194(3) (2011) 459-72.

580

581
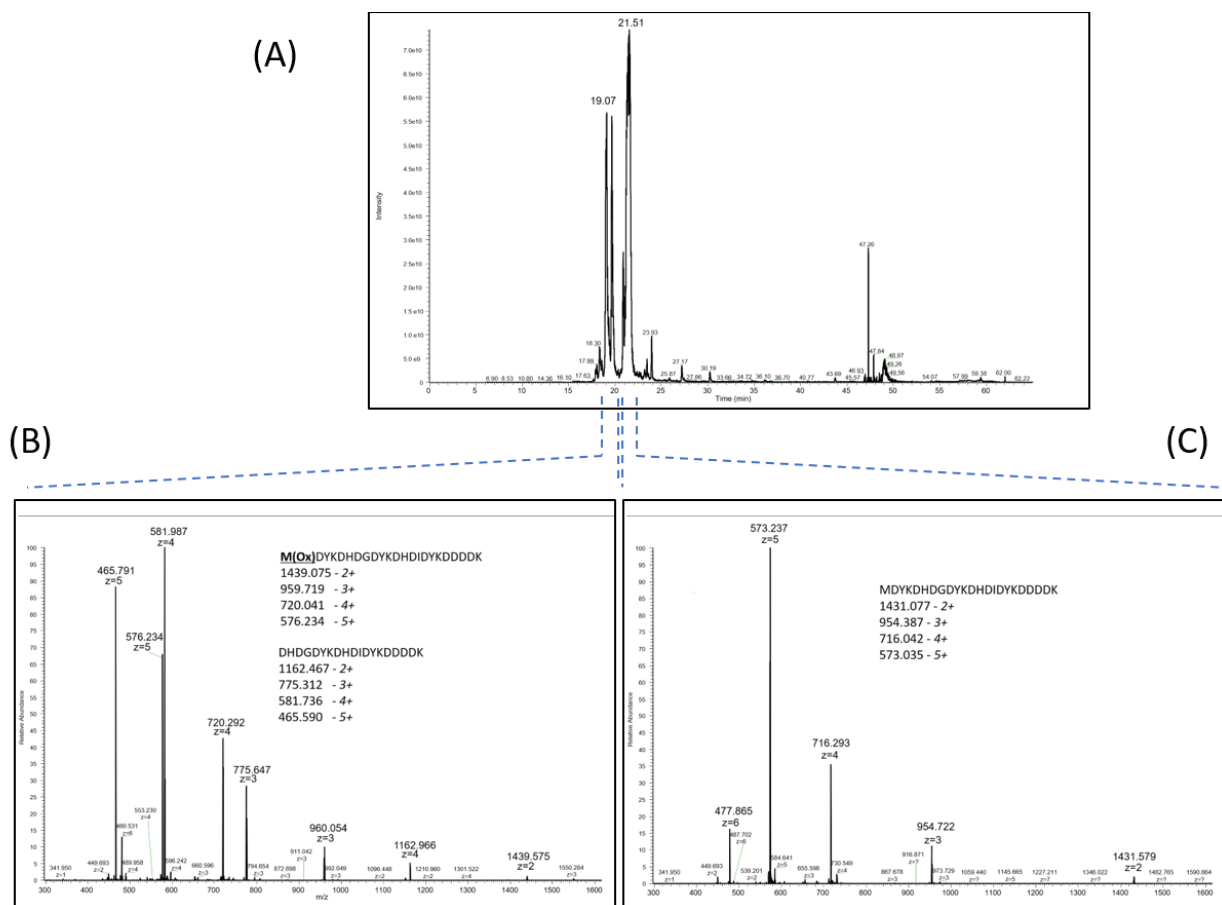
582

583

584 **Figure 1.** A 3X FLAG tag specific Co-IP Mass spectrometry experiment on an Orbitrap Fusion Lumos mass

585 spectrometer. (A) The TIC mass spectrum showing the the most intense peaks between 18-22minutes. (B)

586 The averaged mass spectrum at ~19min showing the presence of the oxidized version of the 3X FLAG

587 peptide and a trypsin derived truncated version of the 3X FLAG peptide. (C) The averaged mass spectrum

588 at ~21min showing the charge distribution of the intact 3X FLAG peptide. Note m/z peak labeling is on the

589 most abundant ion in the isotopic cluster.

590

591

592

593
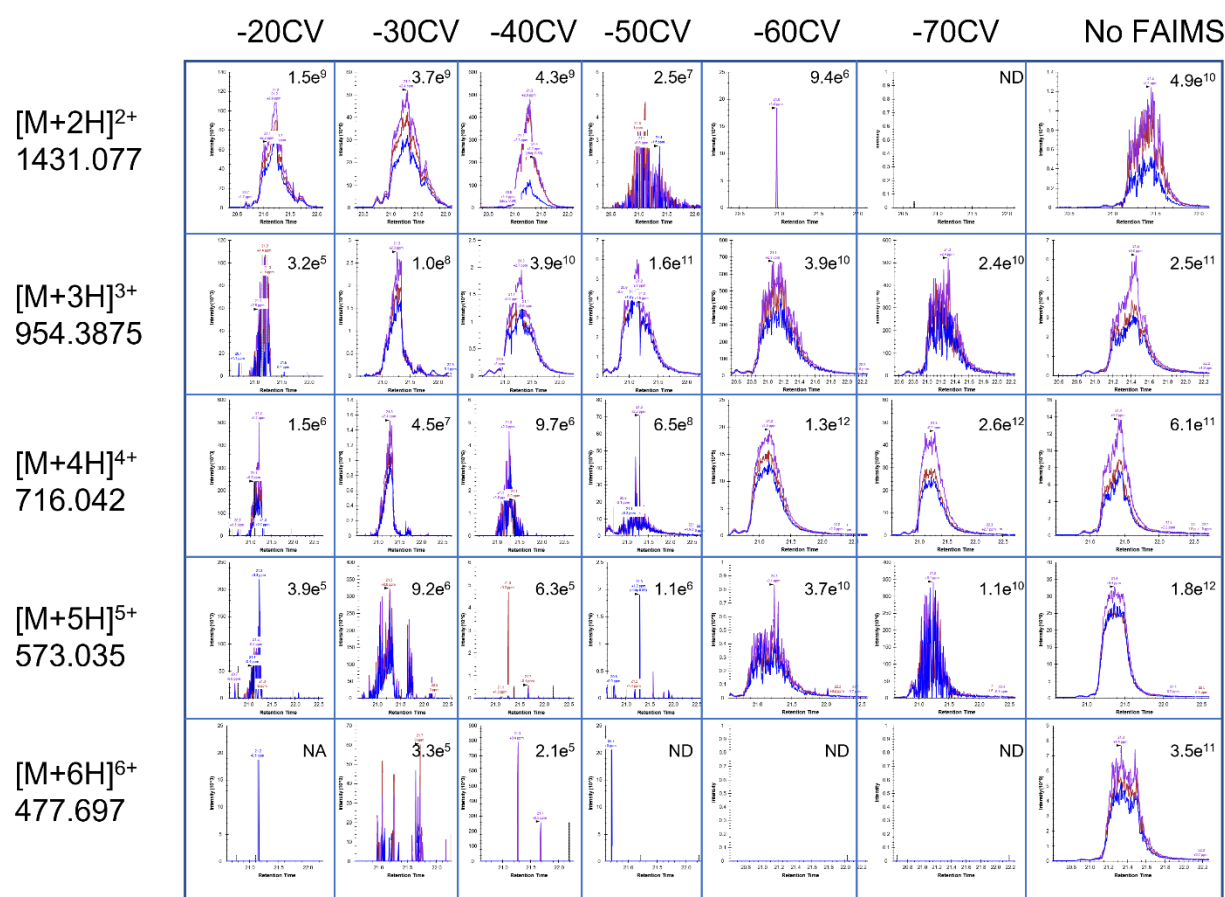
Figure 2: Monitoring the intensities of the different charge species of the 3X FLAG peptide across the different CVs. The extracted ion chromatogram of all graphs is centered at 21.3 min and inserts values represent the total area information. ND = not detected. Metadata is available in Supplementary Table 1.
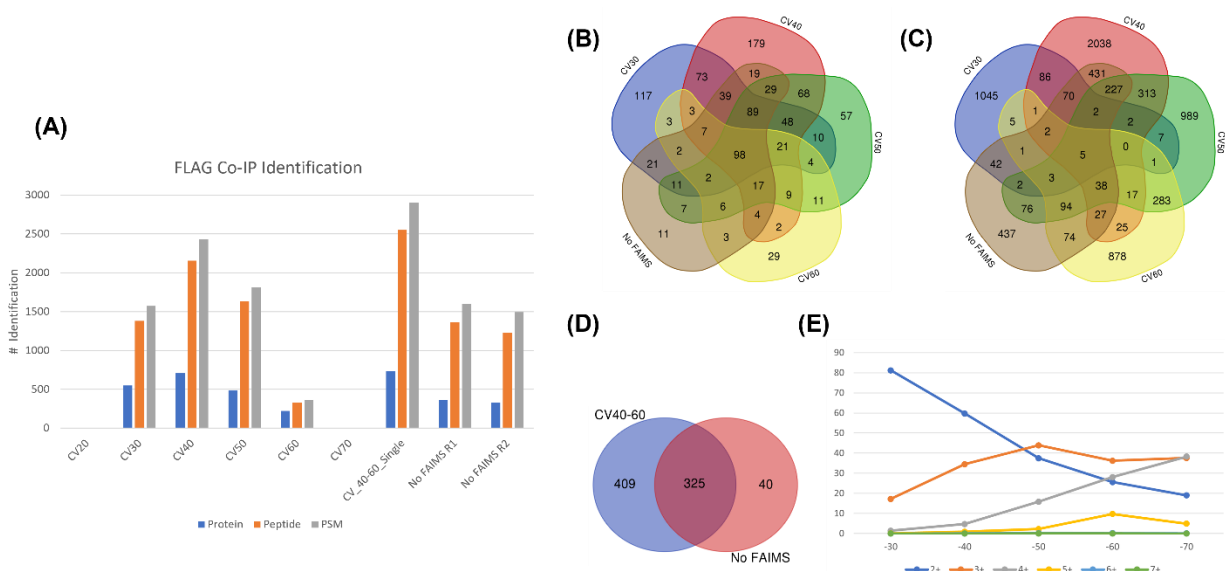
Figure 3. Analyzing the protein and peptide identification from the FLAG Co-IP experiment. (A) Breakdown of protein, peptide and PSM across 6 different CVs, two internal CV stepping and two replicates without FAIMS. We did not identify any proteins with CV-20 and CV-70. (B) Venn diagram of unique protein identification across 4 different CVs (-30, -40, -50 and -60) with No FAIMS applied. (C) Venn diagram of unique peptide identification across 4 different CVs (-30, -40, -50 and -60) with No FAIMS applied. (D) Proteins that are uniquely identified with 2 internal CV stepping vs without FAIMS (E) Charge distribution of MS1 precursors selected for MSMS across the 6 different CVs.
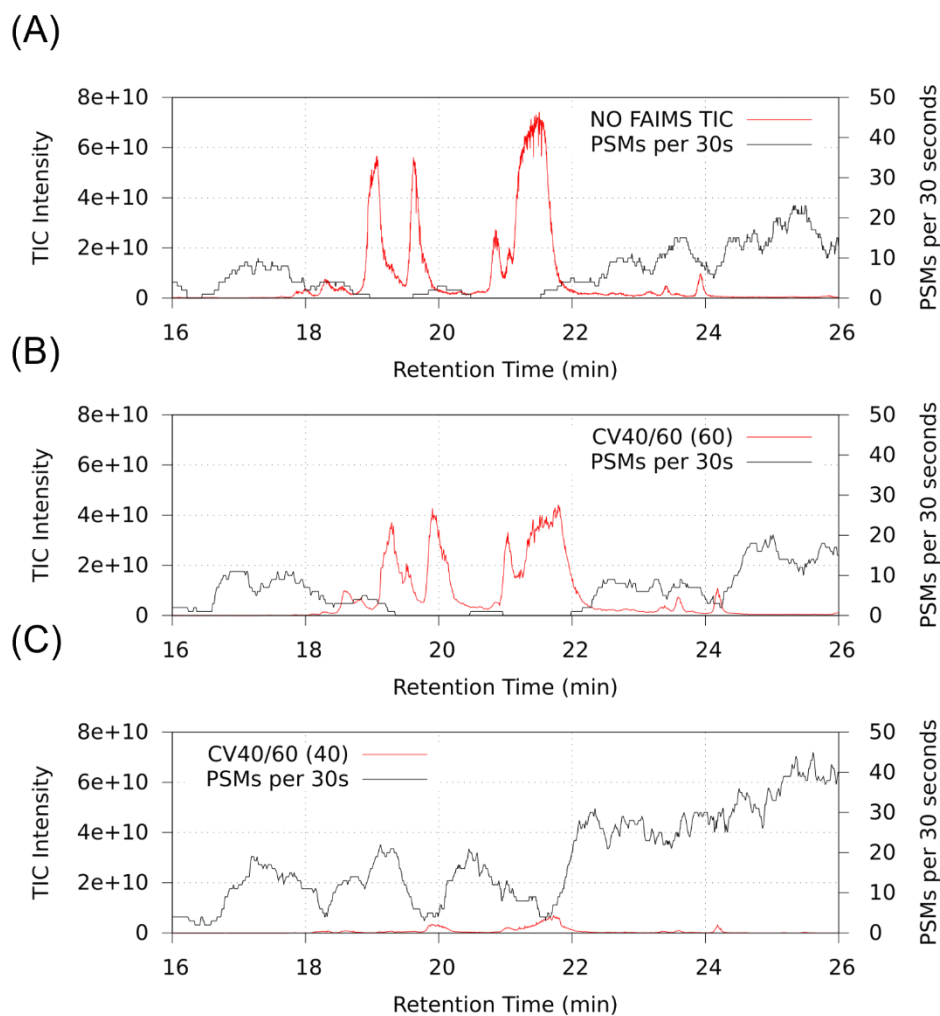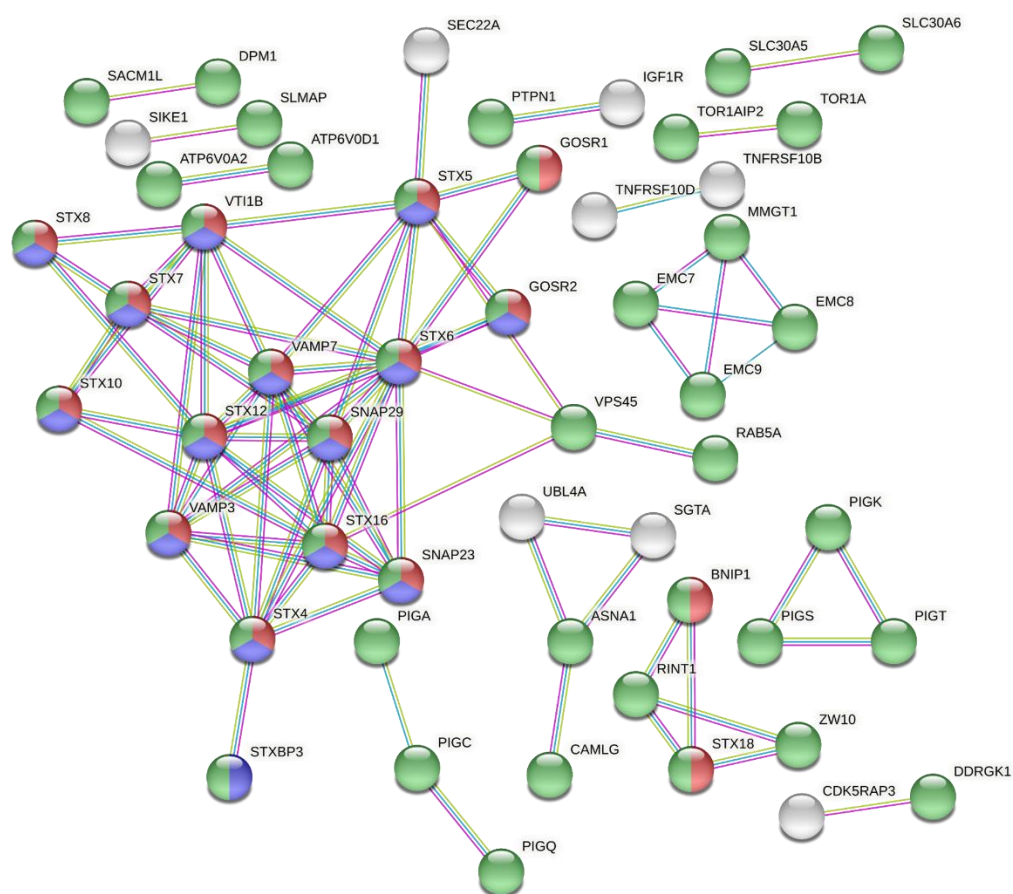
Figure 4: Plot of total ion chromatogram (red trace) and PSM identification (black trace) from the FLAG-Tag Co-IP experiment with (switching between CVs of -40 and -60) and without FAIMS at retention time 16 to 26 min. (A) Experiment without FAIMS (B) Extracted TIC and PSM with FAIMS at CV-60 (C) Extracted TIC and PSM with FAIMS at CV-40.

(A)
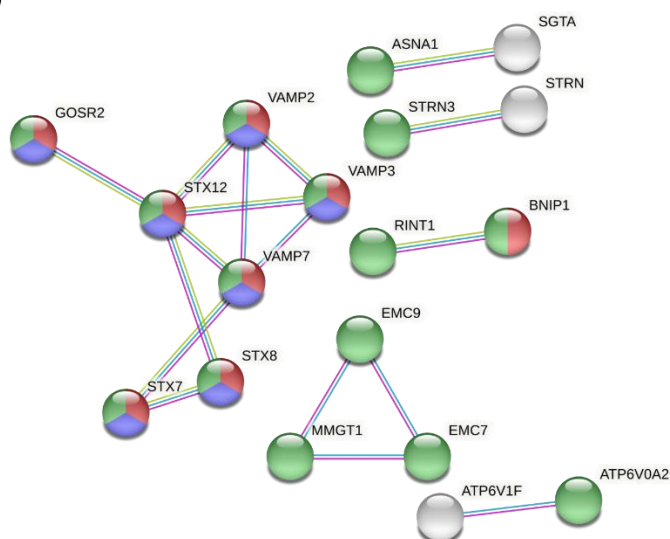
(B)

(C)

(D)

612

613

(E)

614
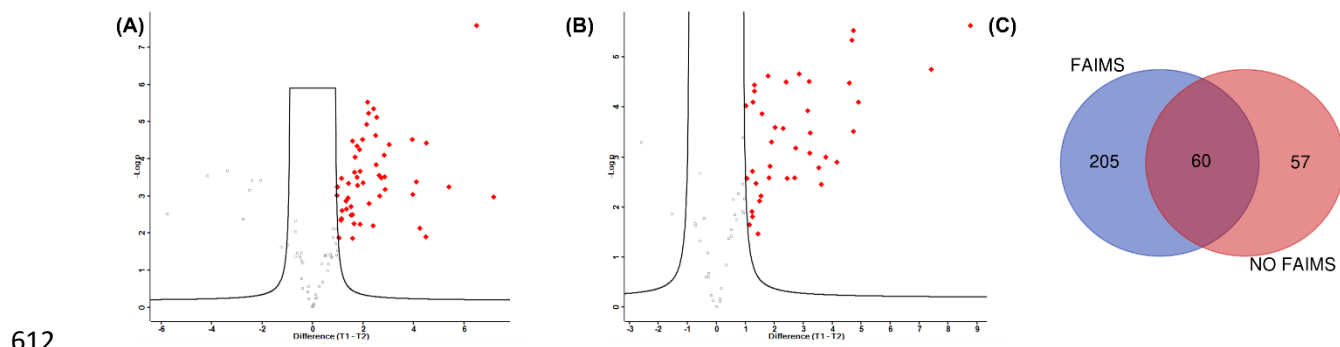
Figure 5: Protein-protein interaction from Co-IP with and without FAIMS (A) Volcano plot from the FAIMS enabled experiment and highlighting proteins (red diamond) that have significantly increased in abundances in drug treated samples (proteins identified in 3 replicates, T-Test, FDR 0.05 and S0=2). X-axis represents log2 transformed fold change and y-axis represents the T-test p values. (B) Volcano plot from the without FAIMS experiment and highlighting proteins (red diamond) that have significantly increased in abundances in drug treated samples (C) Venn diagram of proteins submitted to STRING analysis. These include proteins significantly increased and proteins exclusively found in the drug treatment groups (identified in all 3 replicates of the drug treated group and absent in the other group). (D) STRING physical subnetwork analysis for the FAIMS enabled experiment. For clarity, disconnected nodes have been hidden. Red and blue bubble represent molecular functions enriched in SNAP receptor (p-value = 5.14e-16) and SNARE binding activity (p-value = 3.56e-08), respectively. Green bubble represents enrichment in the endomembrane system (p-value = 1.53e-61). (E) STRING physical subnetwork analysis for without FAIMS experiment. For clarity, discontinued nodes have been hidden. Red and blue bubble represent molecular functions enriched in SNAP receptor (p-value = 2.11e-08) and SNARE binding activity, respectively (p-value = 0.0015), respectively. Green bubble represents enrichment in the endomembrane system (p-value = 1.73e-31). Edges color legend: Pink = experimentally defined, Magenta = from curated databases and Light Green = text mining

632

29